Concentration-Encoded Molecular Communication in Nanonetworks. Part 2: Performance Evaluation

Mohammad Upal Mahfuz, Dimitrios Makrakis and Hussein T. Mouftah

Abstract As discussed in the previous chapter, concentration-encoded molecular communication (CEMC) is an information encoding approach to molecular communication (MC) where a transmitting nanomachine (TN) encodes information by varying the transmission rate of molecules, and correspondingly, a receiving nanomachine (RN) decodes the transmitted information by observing the concentration of information molecules available at the RN. While the previous chapter basically dealt with the fundamentals, issues, and challenges of CEMC system, the main objective of this chapter is to particularly focus on performance evaluation of CEMC system in detail. Understanding a single CEMC link completely and accurately is of utmost importance in order to fully understand CEMC-based molecular nanonetworks in the emerging biological information and communication technology (bio-ICT) paradigm. Hence this chapter focuses on the performance evaluation of a single-link CEMC system between a pair of nanomachines.

Keywords Molecular communication · Concentration encoding · Performance evaluation · Bit error rate · Biological nanomachines · Nanonetworks · System design · Signal detection

Acronyms

ASK	Amplitude-shift keying
BER	Bit error rate

This research work was completed while M.U. Mahfuz was with the University of Ottawa, Canada.

M.U. Mahfuz (✉)
Department of Natural and Applied Sciences (Engineering Technology), University of Wisconsin-Green Bay, 2420 Nicolet Drive, Green Bay, WI 54311, USA
e-mail: mahfuzm@uwgb.edu

D. Makrakis · H.T. Mouftah
School of Electrical Engineering and Computer Science, University of Ottawa, 800 King Edward Ave, Ottawa, ON K1N 6N5, Canada

J. Suzuki et al. (eds.), *Modeling, Methodologies and Tools for Molecular and Nano-scale Communications*, Modeling and Optimization in Science and Technologies 9, DOI 10.1007/978-3-319-50688-3_2

CEMC	Concentration-encoded molecular communication
CIR	Channel impulse response
CME	Chemical master equation
EM	Electromagnetic
FSK	Frequency-shift keying
FPT	First passage time
IM	Impulse modulation
ISI	Intersymbol interference
LRBP	Ligand-receptor binding process
MC	Molecular communication
M-AM	Multilevel amplitude modulation
M-PAM	Multilevel pulse amplitude modulation
OOK	On-off keying
PAM	Pulse amplitude modulation
RN	Receiving nanomachine
RRE	Reaction rate equations
SCK	Stochastic chemical kinetics
TN	Transmitting nanomachine
VAI	Vibrio fischeri Auto-Inducer
VRV	Virtual receiving volume

1 Introduction

Molecular communication (MC) in general requires interdisciplinary knowledge from several technical fields of study ranging from material science through biophysics and computer science to electrical and communication engineering as well as computer networks. While Chap. 1 provides necessary background information on CEMC, this chapter mainly focuses on the performance evaluation of the same. A transmitting nanomachine (TN) releases information molecules in the propagation medium. Solutions to Fick's laws of diffusion provide us with the average concentration of information molecules available at a receiving nanomachine (RN), which is important in the sense that they help us understand diffusion dynamics and communication range- and rate-dependent characteristics of CEMC system in more detail.

In this chapter, we consider a single CEMC link between a pair of nanomachines in aqueous medium. The system model is presented first by presenting the system components and channel impulse response (CIR) characteristics. Suitable signaling schemes in CEMC are described next by detailing transmission and modulation schemes as well as propagation models. CEMC diffusion dynamics are presented next dealing with the average concentration level of available molecules at the RN, without taking into account the noise due to the uncertainty in propagation and reception. Results on diffusion dynamics using average concentration level based on

Fick's laws provide useful insights to identify average performance of a CEMC system, and therefore, are of significant importance in the complete study of CEMC system. Performance of CEMC system by taking into account the randomness due to uncertainty in diffusion-based propagation and reception are also provided, which includes receiver models suitable for CEMC signal detection and analyses in terms of bit error rate (BER) performance and ligand-receptor binding process (LRBP).

Performance evaluation of CEMC system is a wide area open for research at this moment of time. Here in this chapter our focus is on CEMC system based on ideal (i.e. free) diffusion of information molecules. In the simplest form, we assume that propagation medium composes of solvent and information molecules only. Information molecules are of larger size than solvent molecules and collide with solvent molecules randomly and, therefore, become available at the RN in a probabilistic manner. The performance of CEMC system is evaluated by transmitting a random sequence of bits. Communication range varies from several hundreds of nanometres to several tens of micrometres. The effect of intersymbol interference (ISI) is one of the major concerns in CEMC system, which degrades BER performance of the system severely, especially when communication range and/or transmission data rate need(s) to be increased. Effects of ISI have been described in detail. Finally, the findings are summarized with directions to possible future works on the advancements of CEMC system in molecular nanonetworks.

2 System Model

In this section, we describe the system model in general and the characteristics of the CEMC channel. Referring to Fig. 1 in Chap. 1, the assumptions related to diffusion-based CEMC system have been explained in this section. In order to derive the channel characteristics and diffusion-based noise distribution, we first consider an instantaneous transmission of Q_0 molecules at time $t = 0$ at the TN located at $(0, 0, 0)$. Instantaneous transmission is important because it would provide CIR of the CEMC system. When CEMC channel is fully understood, it would be possible to investigate more into other transmission and modulation schemes, e.g. pulse amplitude modulation (PAM), on-off keying (OOK), and frequency-shift keying (FSK) [1]. In this chapter, we also refer to Fig. 1 in the previous chapter and assume the following in the system.

The TN can precisely control the departure time and the number of molecules. The TN is transparent to the released molecules, meaning that the TN does not affect the movement of the released molecules nor does it react with them.

The molecules undergo ideal (i.e. free) diffusion in the propagation medium in three dimensions. This means that in each dimension in space each of the released molecules has equal probability of taking the next step to the right (forward) or to the left (backward) from its previous position [2]. In addition, the molecules propagate infinitely even after the first hitting time at the RN. The RN can sense the number of molecules available for reception at the RN and the molecules that reach

the RN are not removed from the system [3]. This ensures free diffusion of molecules according to Fick's laws [2, 4] and, therefore, the molecules can be available to the RN multiple times according to the ideal diffusion phenomenon in three dimensions in an unbounded propagation medium.

The medium between the TN and the RN is three-dimensional, with the transmitter located at the origin $(0, 0, 0)$ and the RN at any other location in the three-dimensional space. The location of the RN can be identified by the vector $\vec{r} = \hat{\imath} \cdot x_r + \hat{\jmath} \cdot y_r + \hat{k} \cdot z_r$ that has the origin as the starting point and the location of the RN as the ending point. Here $\hat{\imath}, \hat{\jmath}$, and $\hat{k}$ denote unit vectors in x, y, and z axes respectively, $r^2 = x_r^2 + y_r^2 + z_r^2$ and r is the Euclidian distance between the TN and the RN.

The TN and the RN are synchronized in time [5, 6]. The TN releases a number of molecules of the same type and each of the molecules propagates independently to the RN meaning that for molecules i and j, the paths $B_i(t)$ and $B_j(t)$ to the RN are independent if $i \neq j$. Following ideal diffusion mechanism based on random walk motion [2], RN decodes information symbols by measuring molecular concentration at its receptor's location [7].

In discrete-time random walk model, referring to Fig. 3 in Chap. 1, the step size δ and the time τ a molecule remains in one state before it moves to the next state are constants [2, 4]. Also, movement of a molecule to a new position is statistically independent of its previous movement. This makes the discrete-time random walk model Markovian. The medium is assumed to be homogenous in nature for the information molecules.

Sensing time of RN is much shorter than passage time of a molecule, regardless of whether it is a first passage time (FPT) or a higher order passage time. FPT is the time duration from the release of a molecule at TN to the time instant when the molecule first hits the receptor of RN [8]. Alternatively, FPT can also be termed as the propagation delay. Higher order passage times indicate scenarios when the molecule reaches the RN multiple times.

RN contains a number of receptors on its surface, see Fig. 1 in the previous chapter. Surrounding the RN we assume a virtual receiving volume (VRV) [3] with the RN located at its centre. Diffused molecules can interact with the receptors and may or may not bind with them according to ligand-receptor binding process (LRBP) that depends on the affinity of information molecules to the receptors on the surface of the RN. In general, we consider available molecules at the location of the RN with and without LRBP.

2.1 System Components

As shown in Fig. 1 in the previous chapter, a generic CEMC system between a pair of nanomachines consists of a TN, an RN, and a propagation medium between them. The propagation medium can also be thought of as "channel" [9] in similarity with the traditional wireless communication systems [10]. TN transmits information

molecules at a given rate. Examples of information molecules are proteins and ions that contain information to be transmitted. Examples of propagation medium are water ($D = 10^{-6}$ cm^2/s), air ($D = 0.43$ cm^2/s), and blood plasma ($D = 2.2 \times 10^{-7}$ cm^2/s for simple message and 1×10^{-9} cm^2/s for complex message) [11]. Both TN and RN are artificial devices or modified biological cells [12]. RN can receive information molecules at its receptors.

While in the propagation medium there may exist other molecules that may cause undesired chemical reactions [13] and thus may create noise in the system, we have not considered such cases in our research and so in the system model presented in this chapter we consider that the propagation medium consists of solvent molecules only through which the information molecules diffuse and ultimately reach the RN probabilistically. It should be noted that information molecules (e.g. protein, ion) are different from solvent molecules (e.g. water, air, blood plasma) and of larger size than the solvent molecules.

2.2 CIR Characteristics: Distance and Temporal Dependence

The impulse response of CEMC channel needs to be investigated in order to find output concentration of molecules at the location of RN. As shown in the previous chapter, CIR $g(r, t)$ is a function of both time t and TN-RN distance r. Investigating into $g(r, t)$ it is clear that, unlike EM wave-based propagation, modeling CEMC channel cannot be explained in terms of separate distance dependence and temporal dependence. For instance, the exponent part in the expression of $g(r, t)$ is a function of both distance r and time t. In free space, EM waves propagate at the speed of light (3×10^8 m/s). In some cases, wireless channels are realistically assumed to be stationary for short propagation times between sender and receiver. But unlike EM wave propagation, molecular propagation is a very slow process and so spatiotemporal variation of CIR should be investigated in-depth even for short distances [14]. Spatiotemporal variation rather plays a significant role in terms of the analyses of path-loss and output signal. As mentioned earlier, the concentration of molecules at a distance r and at time t, $U(r, t)$, is the intensity [7] of molecular concentration signal at RN. Therefore, any integral of $U(r, t)$ over time would indicate the strength (or, alternatively, energy) [7] of CEMC signal. CIR $g(r, t)$ is normalized to its total energy (i.e. strength) over the entire observation time as $g(r,t)/\int_0^{T_{\text{obs}}} g(r,t)dt$ [15] where, in ideal case of diffusion of molecules, $T_{\text{obs}} = \infty$; however, in numerical simulations, $T_{\text{obs}} = 1$–10 h should be reasonable enough to study the performance of CEMC systems. Figure 1 below shows the energy-normalized CIR $g(r, t)$ at TN-RN distances of 800 nm and 100 μm in water medium. As shown in Fig. 1, CIR becomes temporally spread when r increases causing ISI in signal detection [16–18]. A comparison of the characteristics of CIR of CEMC channel at different TN-RN distances in air medium can be found in [9] whereas the performance of CEMC

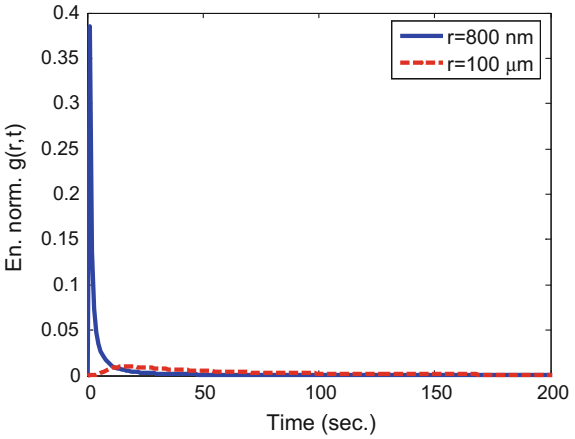

Fig. 1 CIR of CEMC channel in water medium

system based on binary pulse transmission scheme in air, water, and blood plasma propagation media can be found in [16]. Figure 1 is similar to Fig. 5 in the previous chapter in the sense that they both show temporal spreading of CIR. However, Fig. 1 shows the temporal spreading of CIR over an extended time scale up to 200 s and an increased communication range of 100 μm.

3 Transmission and Modulation Schemes

In the transmission phase of CEMC, the TN releases molecules in the propagation medium. The transmission rate, or in other words the concentration of molecules at the TN, can be varied in several ways based on the characteristic feature of the concentration signal at the TN. In the following, we focus on three commonly used modulation schemes in CEMC.

3.1 Impulse Modulation

In impulse modulation (IM), the TN releases all the molecules as an impulsive manner at the beginning of each symbol. Two different schemes, namely, generalized ASK-based and on-off keying (OOK) schemes can exist in IM. In generalized ASK scheme, as shown in Eq. (1), the TN transmits $Q_1\delta(t)$ and $Q_0\delta(t)$ molecules when it wants to send a bits[1] 1 and 0 respectively [19], where $Q_1 \gg 1, Q_0 \gg 1$, and $\delta(t)$ is the Dirac delta function [20] and $Q_1 > Q_0$ in general.

[1]In binary scheme, each symbol is represented as a bit (1 or 0), while in M-ary scheme, each symbol composes of $\log_2 M$ bits [1].

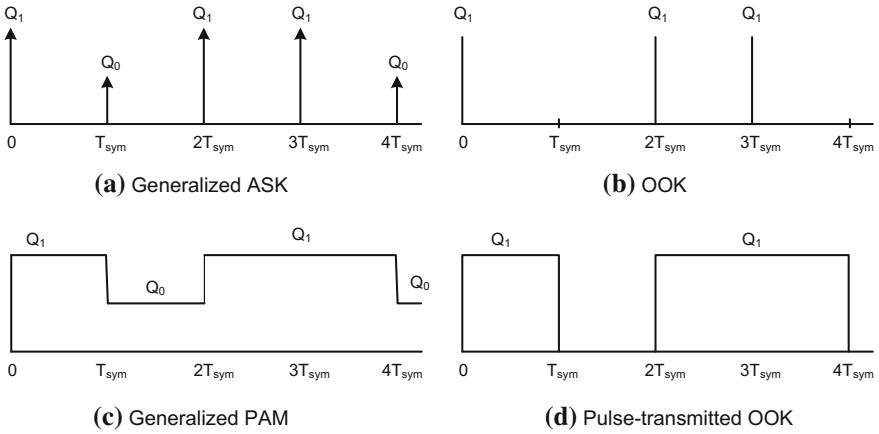

Fig. 2 Generalized ASK and OOK transmission schemes: IM in (**a**) and (**b**), PAM in (**c**) and (**d**). For PAM, $T_p = T_{sym}$ is assumed

$$s(t) = \begin{cases} Q_1\delta(t) & \text{Bit 1} \\ Q_0\delta(t) & \text{Bit 0} \end{cases} \tag{1}$$

However, in OOK scheme, as shown in Eq. (2), the TN sends Q_1 molecules, where $Q_1 \gg 1$, when it wants to send bit 1 and does not send any molecules at all when it wants to send bit 0, meaning that the TN remains apparently in "on" and "off" states while transmitting bits 1 and 0 respectively. Figure 2a, b show ASK and OOK schemes based on IM in CEMC.

$$s(t) = \begin{cases} Q_1\delta(t) & \text{Bit 1} \\ 0 & \text{Bit 0} \end{cases} \tag{2}$$

3.2 Pulse Amplitude Modulation

Pulse-based transmission of molecules in CEMC system is also possible. Unlike impulsive transmission, in pulsed transmission, the TN sends a pulse of molecules with a given pulse-width $0 < T_p \leq T_{sym}$ where T_{sym} denotes the symbol interval. A given T_{sym} determines the separation between the starts of two consecutive pulses of molecules representing two different symbols, and so, T_{sym} determines the effective data rate Ω of the CEMC system as $\Omega = 1/T_{sym}$. Like in conventional communication systems, in CEMC it is also desired to have a higher transmission data rate in order to increase the speed of communication, which faces a challenge in providing reliable CEMC with lower BER between nanomachines while

minimizing the effects of ISI. Like in impulsive transmission, it is also possible to have generalized ASK and OOK schemes both based on pulse transmission. In pulse-based ASK scheme, the TN sends pulses of two different amplitudes to represent the bits 1 and 0. Equation (3) expresses the signal for each symbol when ASK-based transmission is adopted, where $Q_1 \gg 1, Q_0 \gg 1$, and $\Pi(t)$ denotes a rectangular pulse with unity amplitude. The amplitude of the pulse $\Pi(t)$ is unity from $t = 0$ to $t = T_p$ and 0 everywhere else.

$$s(t) = \begin{cases} Q_1\Pi(t); & \text{Bit 1} \\ Q_0\Pi(t); & \text{Bit 0} \end{cases} \tag{3}$$

On the other hand, OOK scheme is a special case of ASK scheme when $Q_0 = 0$. As shown in Eq. (4), in pulse-based OOK, the TN sends a pulse of molecules only to represent bit 1 and does not send any molecules to represent bit 0 and, hence, it apparently remains "off" to represent bit 0. A detailed account of pulse-based modulation schemes in CEMC can be found in [7, 16–18, 21]. Figure 2c, d show pulse-based transmission schemes in CEMC.

$$s(t) = \begin{cases} Q_1\Pi(t); & \text{Bit 1} \\ 0; & \text{Bit 0} \end{cases} \tag{4}$$

3.3 Multilevel Pulse Amplitude Modulation

By varying the number of molecules transmitted by the TN, it is possible to design a multilevel pulse amplitude modulation (M-PAM) scheme based on generalized ASK. In M-PAM, the TN transmits each symbol by using one of the M different transmitted numbers of molecules, meaning that each symbol can be represented by $\log_2$ M bits being transmitted [17]. It is also possible to implement multilevel amplitude modulation based on IM scheme. Transmitted signals in M-PAM can be expressed as shown in Eq. (5) below.

$$s(t) = Q_m\Pi(t), \text{ where } m = \{1, 2, 3, \ldots, M\} \text{ and } Q_m \gg 1. \tag{5}$$

3.4 Sinusoidal Transmission

While IM, PAM, and M-PAM modulation schemes are all based upon varying the amplitudes of the transmitted number of molecules, it is also possible to vary the rate of change of the sinusoidal variation of molecular transmission rate, thereby making it possible to design frequency-shift keying (FSK) modulation in CEMC [14]. Transmitted signals in sinusoidal-based transmission can be expressed as below.

$$Q(t) = Q_{\text{average}} + Q_{\text{amp}} \sin(2\pi ft) \tag{6}$$

Here Q_{average}, Q_{amp}, and f denote average value, amplitude, and frequency of sinusoidal transmission respectively. Since concentration of molecules can never be a negative number, in Eq. (6), $Q_{\text{average}} \geq Q_{\text{amp}}$. In Eq. (6), different information symbols can be encoded by varying either of Q_{average}, Q_{amp}, f, or any combination of these quantities. Based on sinusoidal signaling, varying Q_{average} and/or Q_{amp} would give multilevel amplitude modulation based on sinusoidal transmission, while varying f would give FSK scheme [16, 22].

4 Fick's Laws Diffusion Dynamics

In CEMC, amplitude and frequency (i.e. the rate of change of amplitude) of the concentration signal are two important quantities of the transmitted signal that can be varied in order to materialize various modulation schemes as shown in Sect. 3. As shown earlier, in IM and PAM, information symbols are represented by the number of transmitted molecules at the beginning of symbol interval by following impulsive and pulsed transmissions respectively. On the other hand, in order to represent different symbols FSK-modulated signaling in CEMC relies on varying the frequency of amplitude variation of information molecules at the TN. In this section, based on Fick's laws of diffusion, we focus on mean concentration of molecules at the location of RN.

4.1 Fick's Laws Concentration Channel

Fick's laws of diffusion have been widely known for a long time [23, 24] and express the mean concentration of information molecules that become available at RN through propagation by the means Brownian motion [4]. In ideal diffusion, it is assumed that the total number of molecules is conserved, i.e. no molecules are created or destroyed, which provides us with the probability of having a molecule available at the RN as shown in Sect. 4 in the previous chapter. Several works that focus on the concentration channel based on Fick's laws are reported in [9, 16, 25].

4.2 Pulse-Transmitted Scheme

4.2.1 Single Pulse Transmission

In pulse-transmitted CEMC system, in order to understand the performance of transmitting a bit sequence completely, it is necessary to first understand the

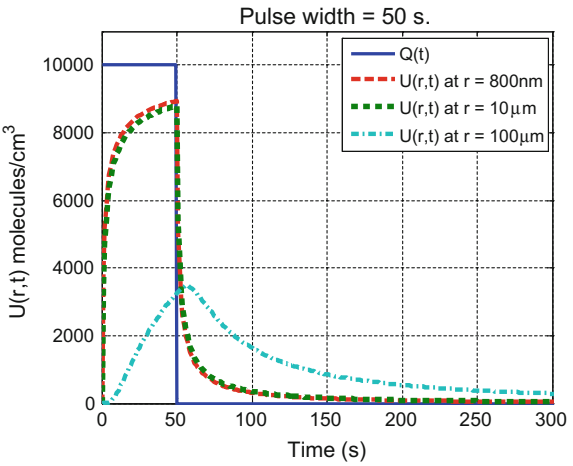

Fig. 3 Available concentration signal intensity at the RN in response to a pulse transmission of pulse-width of 50 s (i.e. data rate $\Omega = 0.02$ bps) in water medium (adapted from [26])

performance of transmitting a single pulse in CEMC channel. Figure 3 shows the output signals at various communication ranges when a single pulse with pulse-width 50 s is transmitted by the TN. As shown in Fig. 3, when communication range increases, signal gets temporally spread and thereby causes an increased level of ISI at the current symbol.

The performance of a pulse transmission can be explained on the basis of *desired signal strength ratio* $S_{(r,f)}$ and *interference strength ratio* $I_{(r,f)}$ expressed as shown in Eq. (7), where E_S, E_U, and E_I are *received desired signal strength*, *received total signal (i.e. desired and interference signals) strength*, and *received interference signal strength* respectively [7].

$$S_{(r,f)} = \frac{E_S}{E_U} = \frac{\int_0^{T_{\text{sym}}} U(r,t)dt}{\int_0^{T_{\text{obs}}} U(r,t)dt} \text{ and}$$
$$I_{(r,f)} = \frac{E_I}{E_U} = \frac{\int_{T_{\text{sym}}}^{T_{\text{obs}}} U(r,t)dt}{\int_0^{T_{obs}} U(r,t)dt} = \frac{(E_U - E_S)}{E_U} = 1 - S_{(r,f)} \tag{7}$$

Here E_S, E_U, and E_I can be found by taking integrals of the output signal $U(r,t)$ over $(0, T_{\text{sym}})$, $(0, T_{\text{obs}})$, and $(T_{\text{sym}}, T_{\text{obs}})$ intervals respectively, as shown in Eq. (7), where T_{sym} and T_{obs} denote symbol duration and observation time respectively.

On the other hand, in case of single pulse transmission, Fig. 4 shows the strength ratio quantities at various communication ranges. When r increases beyond 10 μm, $S_{(r,f)}$ decreases, meaning that the effective desired signal strength decreases. Since at any r and f, $S_{(r,f)} + I_{(r,f)} = 1$, when $S_{(r,f)}$ decreases, $I_{(r,f)}$ increases and vice versa.

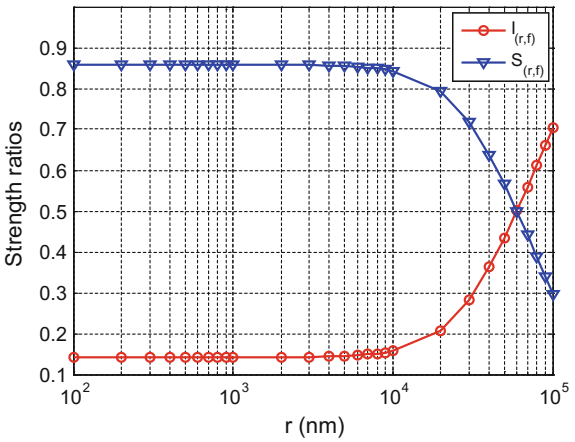

Fig. 4 Strength ratios at various r when pulse-width is 100 s and observation time is 10000 s

A decrease in $S_{(r,f)}$ indicates that more of the output signal strength would be interfering with the detection of the current symbol, and hence an increased level of ISI at the RN.

4.2.2 Bit Sequence Transmission

While the performance of a single pulse transmission provides us with the concepts of desired signal strength and interference signal strength in case of single pulse only, a similar approach can be adopted in pulse-transmitted CEMC scheme in order to send a sequence of bits in the propagation medium. Performance metrics in case of pulse-transmitted OOK-modulated scheme for transmitting a random sequence of bits have been provided in detail in [7]. As shown in Fig. 2d, a TN releases molecules at a fixed rate of Q_1 molecules per second during the entire symbol duration T_{sym} when it wants to send a bit 1 and does not transmit any molecule at all when it wants to send bit 0. Therefore, the entire observation time can be given as $T_{\text{obs}} = NT_b$ where N is the total number of bits to be transmitted and T_b is the duration of each bit in binary CEMC and, therefore, $T_b = T_{\text{sym}}$ in case of binary CEMC system. In case of transmitting a random sequence of bits based on OOK modulation, the signal strengths E_S and E_I can be expressed as the following [7].

$$E_S = \int_0^{T_{obs}} s_{\text{out}}(t)\, dt \quad \text{and} \quad E_I = \int_0^{T_{obs}} i(t)\, dt \tag{8}$$

Here the signals $s_{\text{out}}(t)$ and $i(t)$ in Eq. (8) can be expressed as follows and incorporate the effects of residual molecules originating from the previous symbols that contribute to desired signal strength at the current symbol [7].

$$s_{\text{out}}(t) = \begin{cases} U(r,t) & \text{when } U(r,t) \le Q(t) \\ Q(t) & \text{else.} \end{cases}$$
$$i(t) = \begin{cases} U(r,t) - Q(t) & \text{when } U(r,t) > Q(t) \\ 0 & \text{else} \end{cases} \quad (9)$$

The strength quantities E_S and E_I are very useful in the sense that they can provide us with the techniques to determine effective communication ranges in CEMC [16]. It should be noted here that E_S and E_I provide approximate values of the signal and the interference signal strengths only respectively, and therefore, do not provide accurate estimates of the same [15]. Effective communication ranges for pulse-transmitted CEMC system have been categorized among short, medium, and long ranges in three different types of communication environment, e.g. in air, water, and blood plasma, as reported in [14, 16]. Determining effective communication ranges are important when a nanonetwork of a large number of nanomachines is to be materialized. For example, by computing average concentration of molecules at the RN as found using Fick's laws for pulse-transmitted CEMC, effective communication ranges in water medium can be found as <800 nm for short-range, 800 nm up to 10 μm for medium-range, and >10 μm for long range [16]. Similar short, medium, and long ranges in air can also be found as $r < 0.5$ mm, 0.5 mm $\le r \le$ 1 cm, and $r > 1$ cm respectively [16]. Similarly, short, medium, and long ranges in blood plasma can also be found as $r < 400$ nm, 400 nm $\le r \le 5$ μm, and $r > 5$ μm respectively [16]. The diffusion constants of information molecules in air, water, and blood plasma media, as considered in the determination of effective communication ranges, are 0.43 cm^2/s, 10^{-6} cm^2/s, and 2.2×10^{-7} cm^2/s respectively [11, 16]. Apart from this, as discussed in the previous chapter, increasing effective communication range is highly desired in CEMC. For example, it is shown in [15] that convolutional coding techniques can be applied to pulse-transmitted CEMC systems in order to increase effective communication range. Signal-related quantities when a random sequence of bits is transmitted are shown in Fig. 5.

4.2.3 Communication Range- and Rate-Dependent Characteristics

Communication range and transmission data rate significantly impact the performance of CEMC system. From CIR point of view, when r increases, CIR becomes temporally spread, meaning that in frequency domain amplitude spectrum squeezes. Therefore, fading characteristics of the signal may become affected. However, for lower data rate signals, larger symbol durations can ensure flat fading characteristics on the transmitted signal [10]. This also ensures that all the frequency components of the transmitted signal experience the same fading characteristics in the propagation channel and so the transmitted signal can retain its shape in temporal domain at the RN. While there still exists an open research question on how to select or optimize symbol duration in MC in general, communication range- and

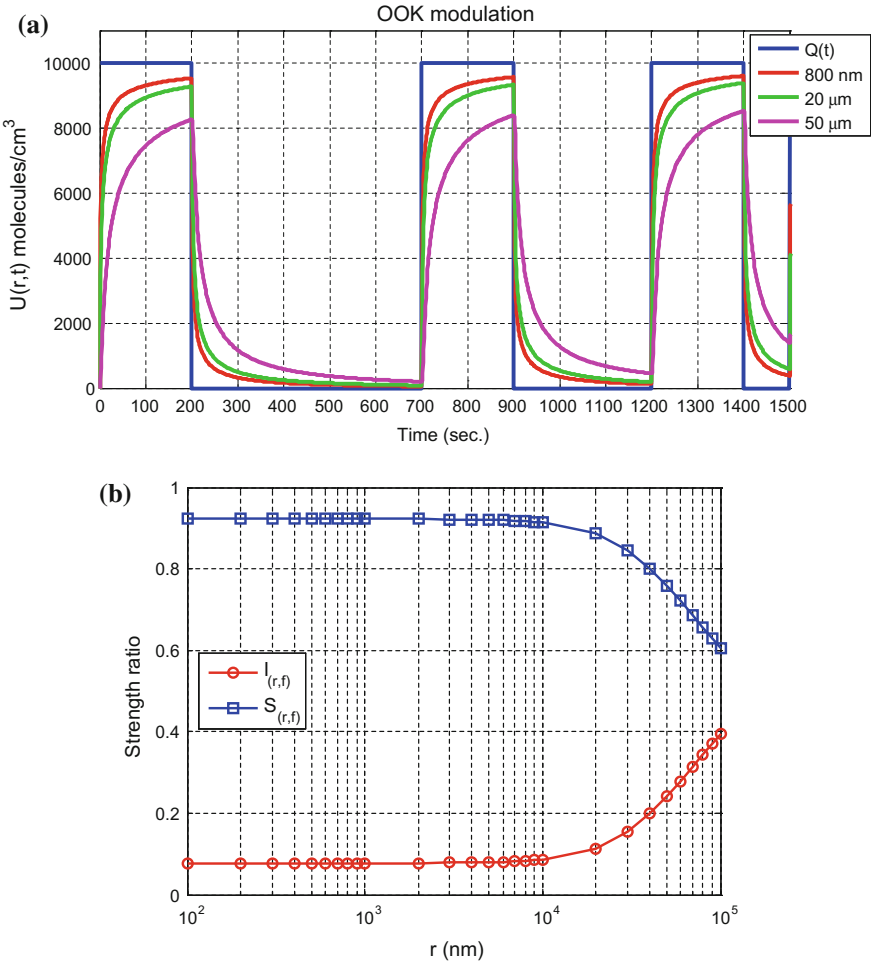

Fig. 5 Transmission of a random sequence of bits in Fick's laws CEMC channel. **a** First 15 bits {110000011000110} of a 100-bit long random sequence of bits is shown where $T_{sym} = 100$ s. **b** Strength ratios when a 100-bit long random sequence of bits with $T_{sym} = 100$ s is transmitted by the TN

rate-dependent characteristics of CEMC systems, especially when a random sequence of bits is transmitted, have been explained in [26].

4.2.4 Multilevel PAM Scheme

In pulse-transmitted CEMC system, it is also possible to develop multilevel PAM scheme based on various amplitudes of the transmitted pulses at the TN [17]. For example, a multilevel amplitude modulation (M-AM) scheme with M = 4, 8, and

16 amplitude levels has been compared with a binary OOK-based scheme in terms of ISI produced by the residual molecules, as reported in [17]. In M-AM, when M increases, due to the higher number of interfering molecules originating from the previous symbols, it becomes very challenging to distinguish the number of molecules corresponding to a given symbol from that corresponding to the remaining symbols and, therefore, BER performance of M-AM system can degrade [15]. At longer communication ranges, a noticeable amount of temporal spreading causes more interfering molecules depending on M-AM level used in the previous symbol. As a result, although total number of accumulated molecules during a symbol increases, BER becomes degraded due to higher level of ISI present during the current symbol. This requires MC engineers to think carefully about effective detection processes of M-AM scheme that would provide low BER at all communication ranges [27].

4.2.5 Reduced Pulse-Width Scheme

In [18], it has been shown that it is possible to design a reduced pulse-width CEMC system by controlling the width of transmitted pulse at the TN. In such a scheme, the TN is assumed to be capable of controlling the pulse-width by deciding on the time instant to stop releasing molecules within each symbol. In general, within each symbol, if a narrower pulse is transmitted instead of a wider one, effective signal strength is found to increase, which should ultimately minimize the effects of ISI on BER. However, in reduced pulse-width-based approach, there arises an issue of reduced signal strength if the pulse-width is reduced without increasing the amplitude of transmitted pulse. There is still room for research on reduced pulse-width scheme for CEMC in nanonetworks [27].

4.2.6 Sinusoidal-Based Signaling

Apart from using pulse-transmitted signaling scheme, it is also possible to design a sinusoidal-based signaling scheme in CEMC [22]. Sinusoidal transmission rates can be expressed as shown in Sect. 3.4. The sinusoidal transmission rate as shown in Eq. (6) can be expressed as the following [22].

$$Q^{'}(t) = \begin{cases} 1 + Q^{'}_{\text{amp}} \sin(2\pi f t) & \text{for } t \geq 0 \\ 0 & \text{for } t < 0 \end{cases} \tag{10}$$

Here $Q'(t)$ and Q'_{amp} indicate transmission rate and amplitude of sinusoidal variation respectively, both normalized to Q_{average}, which results in unitless quantities $Q'(t)$ and Q'_{amp} expressed as $Q'(t) = Q(t)/Q_{\text{average}}$ and $Q'_{\text{amp}} = Q_{\text{amp}}/Q_{\text{average}}$ respectively [22]. Correspondingly, $U'(r, t)$ denotes signal intensity in response to $Q'(t)$, meaning that $U'(r, t)$ is equal to $U(r, t)$ normalized to Q_{average}. The zero initial phase assumption in Eq. (6) allows us to investigate into phase errors in

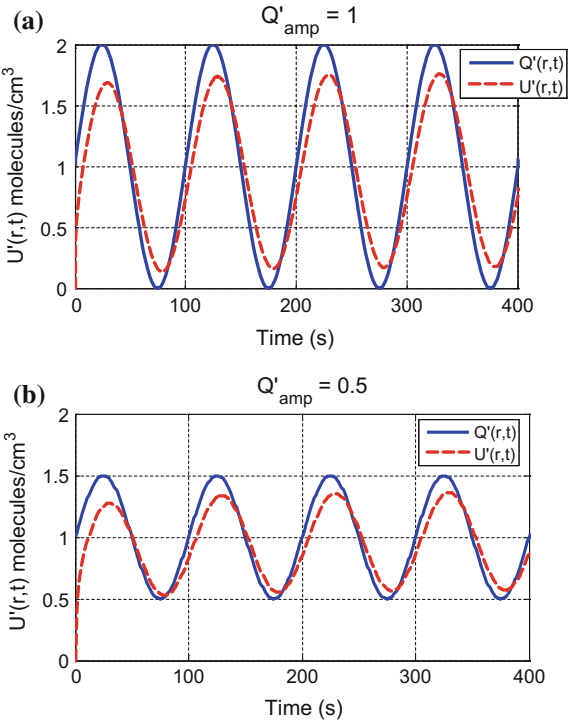

Fig. 6 Output signal intensity $U'(r, t)$ in response to $Q'(t)$ with $f = 0.01$ Hz, $\theta = 0$ rad, and $r = 1$ μm, and **a** $Q'_{\text{amp}} = 1$ and **b** $Q'_{\text{amp}} = 0.5$. Adapted from [22]

sinusoidal-based signaling in CEMC. Figure 6 shows the variation of signal intensity in response to a sinusoidal transmission rate.

Initial and steady-state phase errors, initial and steady-state amplitude losses, and detection noise margin have been explained in [22] using eye-diagram [28] representations as shown in Fig. 7. Results show that even with zero initial phase $U(r, t)$ suffers from phase errors and amplitude loss that vary over communication ranges and transmission data rates as reported in [22]. Transients of phase errors for a given TN-RN pair would also cause problem in the detection of FSK-modulated signals. Figure 7a, b respectively show the eye diagram representations of input $Q'(t)$ and output $U'(r, t)$ signals at the RN. As shown in Fig. 7b, τ_{ini} and τ_{ss} denote initial and steady state phase errors respectively at the RN [22]. In addition, initial and steady state amplitude losses at the RN can be found as below [22], where the quantities c and d can be found as shown in Fig. 7b.

$$AL_{\text{ini}} = 1 - \frac{\text{c}}{Q'_{\text{amp}}} \quad \text{and} \quad AL_{\text{ss}} = 1 - \frac{\text{d}}{Q'_{\text{amp}}} \tag{11}$$

On the other hand, sinusoidal-based signaling can be used in implementing FSK-modulated CEMC. As shown in Fig. 8, a higher frequency sinusoidal signal

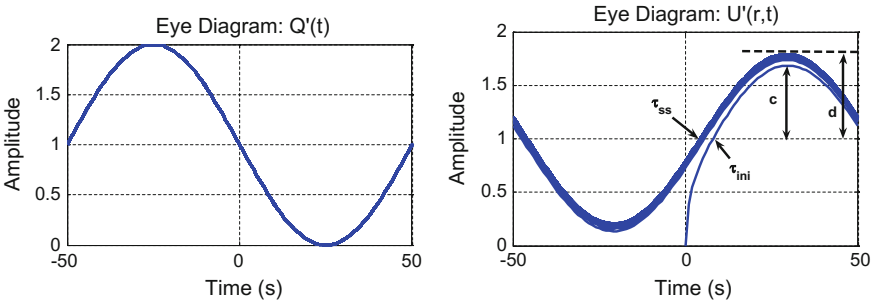

(a) $Q'(t)$ **(b)** $U'(r,t)$

Fig. 7 Representation of input and output signals at $r = 1$ μm using eye diagrams

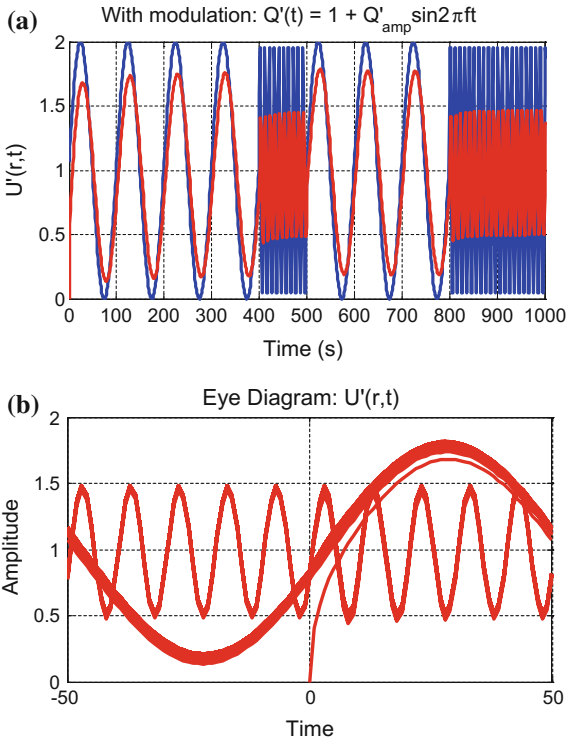

Fig. 8 Input (*blue line*) and output (*red line*) of FSK-modulated CEMC (**a**) and the corresponding eye diagram representation of the output (**b**). Here sinusoidal signals with frequencies $f_1 = 0.1$ Hz and $f_0 = 0.01$ Hz are used to represent bits 1 and 0 respectively, when bit rate $\Omega = 0.01$ bps and $r = 1$ μm

representing bit 1 would experience more amplitude loss at the RN, which would most likely be creating a problem in the detection of output frequency at the RN. In addition to amplitude loss, higher frequency components also experience higher phase errors at the RN [22], which in turn may cause problems in detecting FSK-modulated signals.

5 Signal Detection

5.1 Stochastic Concentration Channel: Signal and Noise Models

The exact number of molecules that become available at the RN at a given time instant is a random variable based on the diffusion-based propagation of molecules. A stochastic channel model takes into account the randomness in propagation in form of diffusion-based noise and ISI [19, 29, 30]. With diffusion-based noise and ISI in effect, in generalized ASK-based transmission scheme as shown in Fig. 2a, the output concentration signal $z(t)$ at time instant t at the RN can be expressed as the following [19].

$$z(t) = s_m(t) + n_s(t) + n_{\text{ISI}}(t) \tag{12}$$

Here $s_m(t)$ is the deterministic part of the signal available in VRV, $m \in \{0, 1\}$, $n_s(t)$ is the diffusion-based noise present at the RN and can be expressed as a zero-mean normal-distributed random variable with variance $s_m(t)(1-p(t))$, i.e. $n_s(t) \sim \mathcal{N}(0, s_m(t)(1-p(t)))$ [19]. Apart from this, $n_{\text{ISI}}(t)$ denotes the residual molecules that cause ISI at the RN and can be expressed as $n_{\text{ISI}}(t) \sim \mathcal{N}\left(\mu_{\text{ISI}}, \sigma^2_{\text{ISI}}\right)$. To incorporate the effects of ISI, μ_{ISI} and σ^2_{ISI} denote the mean and the variance of ISI-producing molecules at the RN respectively. Details of the stochastic CEMC channel model can be found in [19].

Therefore, binary signal detection model in CEMC can be written formally as below

$$z(t) = \begin{cases} \mathcal{N}\left(s_1(t) + \mu_{\text{ISI}}, s_1(t)(1-p(t)) + \sigma^2_{\text{ISI}}\right); & \text{H}_1 \\ \mathcal{N}\left(s_0(t) + \mu_{\text{ISI}}, s_0(t)(1-p(t)) + \sigma^2_{\text{ISI}}\right); & \text{H}_0 \end{cases} \tag{13}$$

where the hypotheses H_1 and H_0 denote the cases when TN sends information bits 1 and 0 respectively; $s_1(t)$ and $s_0(t)$ denote the deterministic mean values of the desired signal at H_1 and H_0 respectively in the absence of diffusion-based noise and ISI, and $p(t)$ is the probability of getting one molecule at the receiver sensing volume VRV.

5.2 Sampling-Based Detection

In sampling-based signal detection, the RN samples the concentration signal intensity at one or more temporal instants in each symbol, and correspondingly, takes decision on which symbol being transmitted based on the sample value(s) of concentration [19]. Communication range-dependent characteristics of sampling-based signal detection show that detection performance becomes improved when

the number of samples taken in each symbol increases [19], meaning that more number of samples provide more information about the transmitted bit, which ultimately help increase the chance of correct detection of the bit under examination. On the other hand, a larger communication range would experience a higher BER due to ISI-producing molecules originating at the previous symbols. However, the capability of the RN of estimating ISI-producing molecules correctly would also be an important factor in order to improve BER performance in such cases. Detection performance also depends on transmission data rate of the system such that at higher data rates BER performance degrades and vice versa. Details on sampling-based signal detection in CEMC can be found in [19].

5.3 Strength-Based Detection

Unlike sampling-based signal detection, in strength-based signal detection the RN accumulates all the molecules that become available at the RN in each symbol and decides on which symbol being transmitted based on comparing the accumulated number of molecules to a threshold [30]. In strength-based detection, after the RN has sensed the intensity of concentration at regular temporal intervals of t_s seconds, it produces as output the detection variable, which can be expressed as below [30],

$$z_{\mathrm{ED}} = s_{\mathrm{ED}} + n_{\mathrm{ED}}^{\mathrm{Noise}} + n_{\mathrm{ED}}^{\mathrm{ISI}} \tag{14}$$

where s_{ED}, $n_{\mathrm{ED}}^{\mathrm{Noise}}$, and $n_{\mathrm{ED}}^{\mathrm{ISI}}$ denote the strengths of desired (deterministic), diffusion-noise, and ISI signals respectively. Since strength-based signal detection can also be thought as energy-based detection [16, 21], here we use the subscript "$_{\mathrm{ED}}$" to denote the quantities related to strength-based signal detection. Therefore, in binary strength-based detection in CEMC, the detection problem can be expressed as below [30], where hypotheses H_1 and H_0 denote transmissions of bits 1 and 0 respectively.

$$z_{\mathrm{ED}} = \begin{cases} \mathcal{N}\left(s_{\mathrm{ED}}^{(1)} + \mu_{\mathrm{ISI(ED)}}, \sigma_{\mathrm{S(ED)}}^{2(1)} + \sigma_{\mathrm{ISI(ED)}}^{2}\right); & \mathrm{H}_1 \\ \mathcal{N}\left(s_{\mathrm{ED}}^{(0)} + \mu_{\mathrm{ISI(ED)}}, \sigma_{\mathrm{S(ED)}}^{2(0)} + \sigma_{\mathrm{ISI(ED)}}^{2}\right); & \mathrm{H}_0 \end{cases} \tag{15}$$

Here $s_{\mathrm{ED}}^{(m)}$ and $\sigma_{\mathrm{S(ED)}}^{2(m)}$, $m \in \{0, 1\}$, denote the deterministic mean signal strength and the variance of diffusion-based noise strength respectively when H_m is true. The quantities $\mu_{\mathrm{ISI(ED)}}$ and $\sigma_{\mathrm{ISI(ED)}}^{2}$ denote the mean and the variance of signal strength arising from ISI-producing molecules. More details of strength-based signal detection in CEMC can be found in [30].

6 Ligand-Receptor Binding

The molecules that become available at RN interact with the receptors located on its surface and based on their interaction the molecules may or may not bind with the receptors. The binding of information molecules with the receptors is commonly known as *ligand-receptor binding*. As mentioned earlier, in CEMC the information molecules are of single type, so are the receptors on the surface of the RN. In general, ligand-receptor binding can be explained by two main approaches, namely, by reaction rate equation (RRE) and by stochastic chemical kinetics (SCK), as described next.

6.1 Reaction Rate Equations

Ligand-receptor binding based on RRE relies on binding and release reactions taking place between information molecules and receptors, where these binding and release reactions are assumed to be taking place only according to the deterministic rates k_+ and k_- respectively [31]. In fact, RREs are a set of coupled ordinary differential equations that explain the temporal evolution of an output (e.g. bound receptors) of a chemical reaction as a deterministic process. In this model, the positions of the receptors and the positions as well as the velocities of the information molecules need to be known accurately in order to derive the temporal evolution of reactions taking place between the information molecules and the receptors. Since it is quite impossible to track the positions and velocities of all the information molecules during a time interval, the temporal evolution of reactions is apparently a non-deterministic process [3], for which the second approach, which is based on SCK, is explained next.

6.2 Stochastic Chemical Kinetics

In SCK approach, the information molecules and the receptors are assumed to form a "well-stirred" system [31], meaning that the locations of the receptors and the information molecules are assumed to be randomly distributed inside the VRV. This allows LRBP to be explained only with the populations of the chemical species, excluding the needs to have the positions of the receptors and the positions as well as the velocities of the individual information molecules to be known as in RRE-based approach. In SCK approach, the number of reactions or the population of each chemical species cannot be known deterministically as in the RRE-based approach, rather probabilistically by using chemical master equation (CME) [3, 31]. In CEMC, realistic channel models have been proposed by incorporating SCK-based approach where the number of reactions that take place within some

time duration is shown to be a Poisson-distributed random variable with rate depending on the propensity function and the time duration [3]. In SCK, propensity function is known as a function that, when multiplied by a time duration, indicates the probability that a reaction would take place between an information molecule and a receptor [3]. Apart from this, the concept of SCK-based approach has been used to design a receiver model for CEMC based on pulse transmission with OOK modulation [26], where the RN is found to develop an optimum receiver based on the average number of molecules that are available for reception at the RN at any symbol incorporating the effects of ISI [26, 32].

7 Conclusion

In this chapter, a thorough investigation has been made into the performance of a diffusion-based CEMC channel where concentration-based approach has been adopted to encode information. CEMC is quite common among biological nanomachines, and therefore, it holds a bright prospect as an information encoding approach in molecular nanonetworks in the future generations of information technology. While MC is gradually maturing and, as a result, progressive works have started to appear in the research community lately, this chapter would be able to provide a good amount of insight to the performance of CEMC system in general. Notable communication features of CEMC, e.g. communication range and transmission data rate, have been investigated from the solutions of Fick's laws that provide average concentration of information molecules at the RN. On the other hand, the roles of diffusion-noise, ISI, and ligand-receptor binding have also been investigated. However, there are several research areas that demand future works in this field to include the following. Optimum signal detectors with sampling-based, strength-based, and SCK schemes for a variety of modulation formats need to be well investigated in order to ensure reliable CEMC for nanonetworks. In addition, the ability of the RN to sense the concentration signal intensity in a more intelligent fashion and correspondingly a formal evaluation of the actual implementation of the optimum signal detector with biological nanomachines should demand more research to be done in this field in the future. On the other hand, intelligent techniques to improve BER at the RN and to increase effective communication range between a pair of nanomachines in a nanonetwork are two areas that are worth investigating in detail in the future. We strongly believe that the investigations into the performance of CEMC system shown in this chapter would encourage interested readers towards new research on CEMC-based molecular nanonetworks and further the knowledge of CEMC in nanonetworks applications in general.

Acknowledgements M. U. Mahfuz would like to thank the Natural Sciences and Engineering Research Council of Canada (NSERC) for the financial support in the form of PGS-D scholarship during the years 2010–2013.

References

1. Haykin S (2000) Communication systems. Wiley
2. Berg HC (1993) Random walks in biology. Princeton University Press, NJ, USA
3. Atakan B, Akan OB (2010) Deterministic capacity of information flow in molecular nanonetworks. Nano Commun Netw 1:31–42, 201003
4. Bossert WH, Wilson EO (1963) The analysis of olfactory communication among animals. J Theor Biol 5:443–469
5. Moore M, Suda T, Oiwa K (2009) Molecular communication: modeling noise effects on information rate. IEEE Trans NanoBiosci 8:169–180
6. Moore MJ, Nakano T (2011) Synchronization of inhibitory molecular spike oscillators. In: BIONETICS-2011
7. Mahfuz MU, Makrakis D, Mouftah HT (2011) A comprehensive study of concentration-encoded unicast molecular communication with binary pulse transmission. In: 2011 11th IEEE conference on nanotechnology (IEEE-NANO), pp 227–232
8. Eckford AW (2007) Nanoscale communication with brownian motion. In: 41st annual conference on information sciences and systems, 2007. CISS'07, pp 160–165
9. Mahfuz MU, Makrakis D, Mouftah HT (2010) Characterization of molecular communication channel for nanoscale networks. In: Proceedings 3rd international conference on bio-inspired systems and signal processing (BIOSIGNALS-2010), Valencia, Spain, pp 327–332
10. Rappaport TS (2002) Wireless communications: principles and practice. Prentice Hall PTR, Upper Saddle River, N.J
11. Lacasa NR (2009) Modeling the molecular communication nanonetworks, MSc thesis, The Universitat Politècnica de Catalunya (UPC), Spain
12. Nakano T, Moore M, Enomoto A, Suda T (2011) Molecular communication technology as a biological ICT. In: Sawai H (ed) Biological functions for information and communication technologies. Springer, Berlin, pp 49–86
13. Moore MJ, Enomoto A, Suda T, Nakano T, Okaie Y (2007) Molecular communication: new paradigm for communication among nano-scale biological machines. In: Bidgoli H (ed) The handbook of computer networks. Wiley
14. Mahfuz MU, Makrakis D, Mouftah H (2010) Spatiotemporal distribution and modulation schemes for concentration-encoded medium-to-long range molecular communication. In: 2010 25th biennial symposium on communications (QBSC), pp 100–105
15. Mahfuz MU, Makrakis D, Mouftah HT (2013) Performance analysis of convolutional coding techniques in diffusion-based concentration-encoded PAM molecular communication systems. BioNanoScience 3:270–284 (Springer)
16. Mahfuz MU, Makrakis D, Mouftah HT (2010) On the characterization of binary concentration-encoded molecular communication in nanonetworks. Nano Commun Netw J 1:289–300 (Elsevier)
17. Mahfuz MU, Makrakis D, Mouftah HT (2011) On the characteristics of concentration-encoded multi-level amplitude modulated unicast molecular communication. In: 2011 24th Canadian conference on electrical and computer engineering (CCECE), pp 000312–000316
18. Mahfuz MU, Makrakis D, Mouftah HT (2011) Characterization of intersymbol interference in concentration-encoded unicast molecular communication. In: 2011 24th Canadian conference on electrical and computer engineering (CCECE), pp 000164–000168
19. Mahfuz MU, Makrakis D, Mouftah HT (213) Sampling based optimum signal detection in concentration-encoded molecular communication receiver architecture and performance. In: Proceedings of 6th international conference on bio-inspired systems and signal processing (BIOSIGNALS-2013), Barcelona, Spain
20. Haykin S (2002) Signals and systems. Wiley, New York
21. Mahfuz MU, Makrakis D, Mouftah HT (2011) On the detection of binary concentration-encoded unicast molecular communication in nanonetworks. In: Proceedings

4th international conference on bio-inspired systems and signal processing (BIOSIGNALS-2011), 26–29 Jan 2011. Rome, Italy, pp 446–449
22. Mahfuz MU, Makrakis D, Mouftah HT (2011) Transient characterization of concentration-encoded molecular communication with sinusoidal stimulation. In: Proceedings of the 4th international symposium on applied sciences in biomedical and communication technologies (ISABEL'11), Article 14, 6 p. Barcelona, Spain
23. Einstein A (1905) On the movement of small particles suspended in stationary liquids required by the molecular-kinetic theory of heat. Ann Phys 17:549–560
24. Philibert J (2006) One and a half century of diffusion: fick, einstein, before and beyond. Diffus Fundam 4:6.1–6.19
25. ShahMohammadian H, Messier GG, Magierowski S (2012) Optimum receiver for molecule shift keying modulation in diffusion-based molecular communication channels. Nano Commun Netw 3:183–195, 201209
26. Mahfuz MU, Makrakis D, Mouftah HT (2012) Strength based receiver architecture and communication range and rate dependent signal detection characteristics of concentration encoded molecular communication. In: Proceedings of BWCCA-2012, Victoria, Canada, pp 28–35
27. Mahfuz MU, Makrakis D, Mouftah HT (2013) Concentration encoded molecular communication: prospects and challenges towards nanoscale networks. In: Proceedings of international conference on engineering, research, innovation and education (ICERIE-2013), Sylhet, Bangladesh, pp 508–513
28. Lee EA, Messerschmitt DG (1994) Digital communication. Kluwer Academic Publishers, USA
29. Pierobon M, Akyildiz IF (2011) Diffusion-based noise analysis for molecular communication in nanonetworks. IEEE Trans Signal Process 59:2532–2547
30. Mahfuz MU, Makrakis D, Mouftah HT (2013) A generalized strength-based signal detection model for concentration-encoded molecular communication. In: Proceedings 8th international conference on body area networks (BodyNets 2013), Boston, MA, USA (30 Sept–02 Oct 2013), pp 461–467
31. Pierobon M, Akyildiz IF (2011) Noise analysis in ligand-binding reception for molecular communication in nanonetworks. IEEE Trans Signal Process 59:4168–4182
32. Mahfuz MU, Makrakis D, Mouftah HT (2014) Strength-based optimum signal detection in concentration-encoded pulse-transmitted OOK molecular communication with stochastic ligand-receptor binding. Simul Model Pract Theor 42:189–209 (Elsevier)